

*Determining Mass Flow Rate of an Electronic Axial Computer
fan from 0.083 to 0.275 slugs/min over 3.466 to 12.59 V Input
Voltage*

November 11, 2022

Ben Salak

Devin Palmer

Jeremy Grubb

Jerritt Gutierrez

ME421 Mechanical Engineering Laboratory

Dr. Ben Mertz



Contents

Abstract	3
Introduction	4
Literature Review	4
Modeling	7
Determining the uncertainty equation for the DRE	9
Creating a preliminary uncertainty budget	9
Apparatus, Procedure, and Design Space Plot	15
Data and Analysis	22
Results and Discussion	28
Conclusion	31
References	32
Appendices	34
Appendix A: Simplifications of the uncertainty equation	34
Appendix B: Testing and Refinement	37
Data collection	37
Shakedown uncertainty	41
Apparatus Refinements	43
Appendix C: Uncertainty in the Integration Method	45
Appendix D: Hotwire Anemometer Calibration and Correction Factor	47
Appendix E: Unprocessed Velocity Data	49
Appendix F: Average Mass Flow Rate Uncertainty Tables and Individual Calculated Mass Flow Rate Uncertainty Tables	61
Appendix G: MATLAB Script used for Post Processing	76

Abstract

Knowing the mass flow rate of air through an axial PC fan is ideal to know for cooling system design to ensure the proper cooling is being provided. This project aims to determine the mass flow rate through an electronic axial computer fan over a range of 0.083 to 0.275 slugs/min with a target uncertainty of $\pm 15\%$. This is justified by the 10% uncertainty in the Wathai 12V fan's volumetric flowrate claimed on the Amazon webpage as well as prior art on mean flow with an uncertainty of $\pm 9.3\%$ [1] [2]. Goals for this experiment include creating a design that minimizes flow losses, achieving a relative uncertainty less than or equal to 15% in the mass flow, as well as to plot the mass flow rate of the fan over the operating voltage range of the fan using the provided voltage controller.

The mass flow rate measurements were accomplished with an apparatus designed for creating a controlled measurement system. The apparatus includes a measuring grid for placing a thermal anemometer into the flow field in certain locations for repeatability of the measurements. This ensured that the anemometer was placed in the same locations for each grid square measured across all trials. The measuring grid also allowed for the use of the equal area integration method outlined in "Equal Area vs. Log-Tchebycheff" with a six-by-six square grid, giving 36 total data points across the measuring area [3]. Along with this, the design also includes a diffuser of one effective duct length long to contain all the air that is pushed through the fan blades. It was determined experimentally with pitot tubes that the pressure drop across the diffuser was negligible, allowing for the assumption that there are no significant losses in the flow while the air is traveling through the diffuser to the measuring grid.

The average relative uncertainty of all the trials conducted turned out to be 4.05%. This was much better than expected and can be contributed to an apparatus that allowed repeatable and stable measurements. The team did find that the measured values generally were a 2% to 26% difference from the datasheet on the Amazon page [1]. The final range of mass flow measured through the fan was 0.083 to 0.275 slugs/min with uncertainties ranging from 2.442% to 3.725% uncertainty in the final measurements.

Introduction

A large portion of electronics use convective cooling (fans that blow cool air onto hot computer parts) to keep the parts at a safe temperature and ensure they do not overheat [4]. When an electronic device like a computer overheats, it can lead to significant damage of the internal components. Convective cooling relies on a fan drawing power and blowing cooler air onto the internal components. This blowing motion takes heat energy from the hot components, causing them to remain cool [4].

If an engineer has a complete understanding of the fan performance, they can efficiently implement the fan in their project using variable power to give just enough cooling to the system. The benefits of using variable speed control on fans include reduced noise, reduced power consumption, and increased fan lifetime [5]. To model the system accurately, the engineer will need to know the relationship between the input voltage and the mass flow rate of the fan. From an experimental design perspective, the motivation can be expanded to include an experiment that can be modified to successfully measure the mass flow rate at varied input voltages on other, different sized fans.

The goal of this project is to determine the mass flow rate through an electronic axial computer fan over a range of 0.0940 to 0.2350 slugs/min with a target uncertainty of $\pm 15\%$. The Amazon page for the Wathai fan used in testing has a relative uncertainty of 10% on the maximum volumetric flow rate value [1]. This 10% margin on maximum volumetric flow rate has been seen on similar sized fans made by Cooler Master [6]. However, with further research into measurement techniques, the target uncertainty for the experiment outlined in this report is $\pm 15\%$. This value was reached after consulting a research paper regarding the uncertainty analysis of mean flow, which concluded with a $\pm 9.3\%$ uncertainty in mean flow [2]. Considering the 9.3% uncertainty from the paper and the 10% uncertainty in the fan's claimed performance metrics, it is reasonable to have a goal uncertainty of 15%.

Literature Review

To calculate the mass flow rate of the fan, the definition of mass flow rate is used. This definition depends on a non-uniform velocity profile that varies with position in the cross section in the flow region:

$$\dot{m} = \oint \rho(\overrightarrow{V_{rel}} \cdot \hat{n}) dA \quad (1)$$

This velocity at specific points in the cross section can be measured using various devices such as ultrasonic flow measurement, particle image velocimetry, pitot tube arrays, and temperature anemometry.

Ultrasonic flow measurement uses time difference to calculate how to measure air flow. A sound wave is sent in the direction against the flow and then returned to the sensor. The difference in the transit time across the air is proportional to the flow rate of the medium [7]. The benefits of ultrasonic measurement are that it has few moving parts, is portable, and is accurate [7].

Particle image velocimetry (PIV) is a method that can be used to measure the velocity profile of a fluid. PIV is often used to validate computational fluid dynamics (CFD) models since it is unobtrusive to the flow [8]. A laser and cameras are used to track marker particles that are placed in the flow. The research paper “Accuracy of volumetric flow rate inflow/outflow measurements by integrating PIV velocity fields,” used two cameras and was able to reach a final highest uncertainty of 4% [8]. PIV experiments tend to always have biases in data since the particles being tracked are extremely small and are tracked over very short distances and periods of time [8].

Another possible method of measuring velocity is by using a “Wilson flow grid”. This method consists of creating a grid of pressure sensors across the area of the pipe. Each sensor has a static and a stagnation port- essentially functioning as a pitot tube. The sensors measure the difference in these pressures, which is then used to find flow speed at each point. From there the average speed can be calculated throughout the entire area. It is important to note that the presence of the sensors in the pipe obstructs the fluid flow causing the air to speed up around the sensors, which, in turn lowers the static pressure more than it would be without the sensor there [9]. Airflow, a company that produces sensors and Wilson flow grids, reports the accuracy of these systems to be as low as 2% [10].

Temperature anemometry can be used to measure an entire velocity profile at any instant instead of having to traverse a probe to different locations into a flow field. Temperature anemometry uses an array of resistors that vary in resistance depending on the temperature. The temperature change is measured by either the voltage or current passing through the resistor [11]. The research paper “Thermal Anemometry Grid Sensor,” lists different methods for doing this. The voltage or current output is then used with the fluid temperature and convection heat transfer principles to determine the speed of the fluid passing over the resistor. This is then extrapolated to a grid format where multiple measurements of the entire flow field can be taken at once [11].

Once the velocity profile has been gathered using experimental data, an integration scheme can be used to solve for the mass flow rate. Integration schemes include equal area method, Log-Tchebycheff method, and diameter bisection method.

The equal area method and the Tchebycheff method are two similar ways to characterize the velocity profile of an air stream through a rectangular duct. According to the journal article “Equal Area vs. Log-Tchebycheff,” both methods divide the cross-section of the duct into parts and a pitot-static tube or other type of pressure probe is then used to measure the pressure of the stream of air at that point [3]. The key difference is how these two methods place the points within the cross-sectional area. In the equal area method, the entire cross section is divided into equal sized rectangles and the measurement point is the center of the rectangles. Depending on the size of the duct, there must be a certain number of rectangles to ensure accurate results. The Tchebycheff method uses percentages of the dimensions of the duct to create a grid. The intersections of the grid are the points where the measurements are taken. Between these two methods, the Tchebycheff method has a higher density of readings towards the middle of the duct and near the walls of the duct, which, makes the velocity profile more accurate [3]. Using one of these schemes allows you to create a two-dimension velocity field which can be used in

the integral definition of mass flow. A research paper stated that depending on the pipe/duct size there is no preference of equal area method or Tchebycheff method since there is only a 3% difference in the velocity profiles made by each method at small duct/pipe sizes [12]. The same research paper stated that the equal area method overestimated the flowrate in a circular pipe by 3.5% to 4.7% while Tchebycheff method was able to reach 0.4% to 0.8% of the actual values [12].

The motivation behind the bisection method is that the Log-Tchebycheff method and the equal area method are too cumbersome to calculate where to place the pitot tube [13]. This becomes apparent when the experiment calls for a change in pipe diameter, which causes a large calculation overhead [13]. The bisection method uses pitot tube measurement points that are positioned at $2^{-1,2,\dots,n}$ from the radius and center of the pipe as shown in Figure 1.

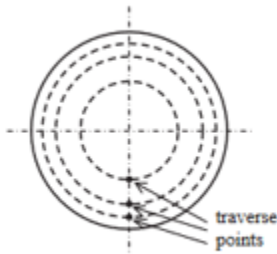


Figure 1: Diameter Bisection method example.

This allows for the measurement scheme to scale well with the varying diameter of the pipe. This scheme does, however, introduce a correction factor because the average velocity is not represented by the velocity at a traverse point. However, the benefits of the bisection method offer more flexibility with the pitot tube points, and there is a smoother error curve [13].

Modeling

To create the equations needed to model the system, consider the following schematic in

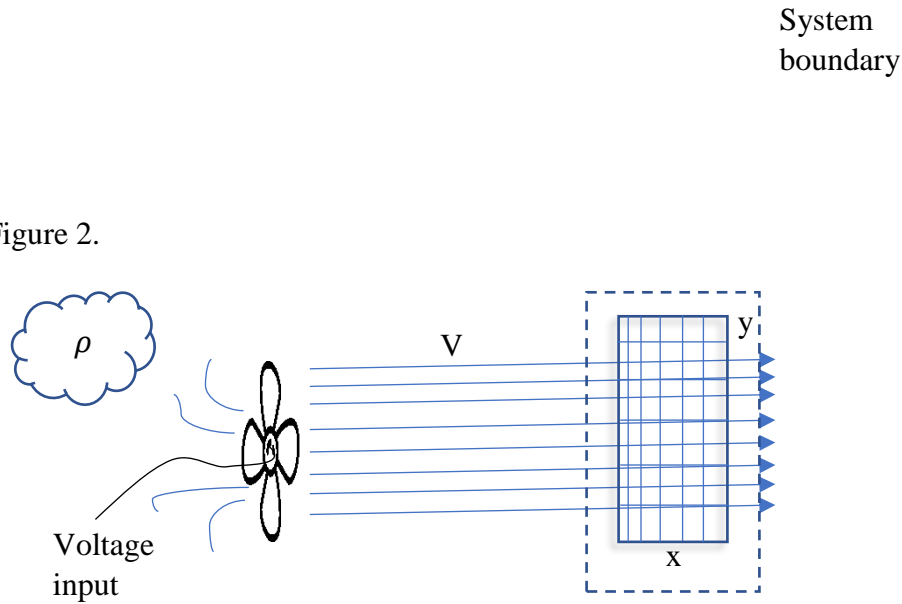


Figure 2: Schematic to analyze mass flow through the system

Using the definition of mass flow rate stated in Equation 1, the integration area can be expanded into x and y coordinates (with flow moving in the z -direction) found in Equation 2.

$$\dot{m} = \oint \oint \rho (\vec{V}_{rel} \cdot \hat{n}) dxdy \quad (2)$$

Where ρ is density of the fluid (air), \vec{V}_{rel} is velocity, \hat{n} is the unit vector normal to the integration area, x is the width of the fan testing area, and y is the height of the fan testing area. To better clarify Equation 1, dx and dy are small segments making up dA . Under the assumption that the flow of air is normal to the fan face the dot product can be evaluated, which leads to Equation 3.

$$\dot{m} = \iint \rho V dxdy \quad (3)$$

Given the flow speeds are at relatively low speeds compared to when flow becomes compressible, it is reasonable to assume that the flow is incompressible, so the density stays constant. This leads to the simplified integral in Equation 4.

$$\dot{m} = \rho \iint V dxdy \quad (4)$$

The rectangular fan can be viewed and subdivided into small dx and dy , or rather Δx and Δy , segments using the equal area method as shown in Figure 3.

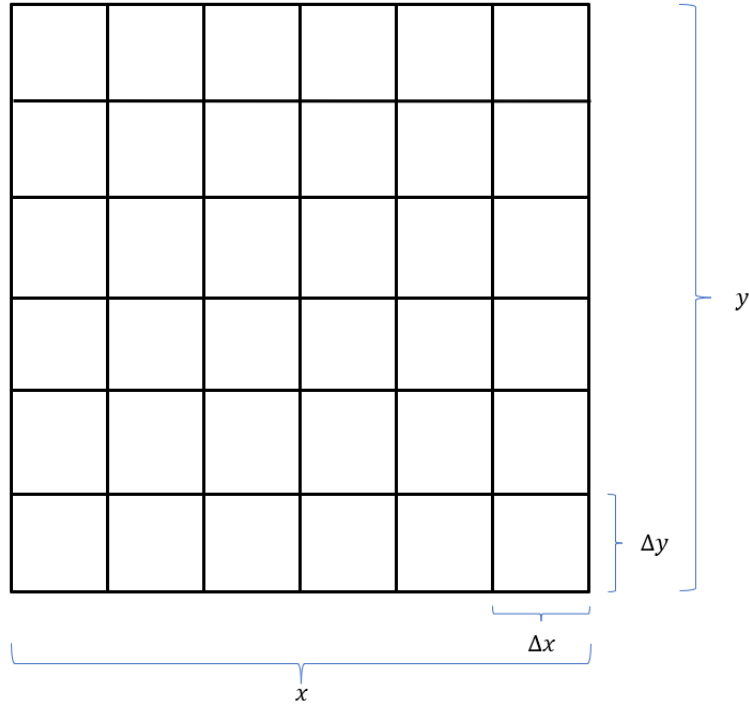


Figure 3: Example of grid view of some testing area of size x by y for an axial computer fan

Since the exact equation for the velocity profile is unknown, the integral can be approximated by taking the sum of velocities in each small equally sized Δx and Δy segment as represented in Equation 5.

$$\dot{m} = \rho \sum_{i=1}^n V_i \Delta x \Delta y \quad (5)$$

Using the assumption of incompressible flow and the ideal gas law shown in Equation 6, the density of air can be represented in terms of atmospheric pressure, P_{atm} , atmospheric temperature, T_{atm} , and the gas constant for air, R .

$$\rho = \frac{P_{atm}}{RT_{atm}} \quad (6)$$

Substituting Equation 6 into Equation 5, the result is Equation 7 below.

$$\dot{m} = \frac{P_{atm}}{RT_{atm}} \sum_{i=1}^n V_i \Delta x \Delta y \quad (7)$$

Since the area being evaluated inside of the summation is equal to the total area of the grid, it can be factored out of the summation as the total test area. The inverse of the number of smaller areas (n) can also be pulled out of the summation since it ends up being one over a constant value. The summation then becomes the sum of all the velocities at the different test points.

Performing these simplifications, the final data reduction equation (DRE) is shown in Equation 8.

$$\dot{m} = \frac{P_{atm}}{RT_{atm}} xy \frac{1}{n} \sum_{i=1}^n V_i \quad (8)$$

Determining the uncertainty equation for the DRE

The uncertainty equation for mass flowrate for the derived DRE is shown in Equation 9 below.

$$\begin{aligned} w_{\dot{m}}^2 &= \left(\frac{\partial \dot{m}}{\partial P_{atm}} \right)^2 w_{P_{atm,sys}}^2 + \left(\frac{\partial \dot{m}}{\partial T_{atm}} \right)^2 w_{T_{atm,sys}}^2 + \left(\frac{\partial \dot{m}}{\partial V_1} \right)^2 w_{V_{1,sys}}^2 + \dots + \left(\frac{\partial \dot{m}}{\partial V_n} \right)^2 w_{V_{n,sys}}^2 \\ &\quad + \left(\frac{\partial \dot{m}}{\partial x} \right)^2 w_{x,sys}^2 + \left(\frac{\partial \dot{m}}{\partial y} \right)^2 w_{y,sys}^2 + w_{integration}^2 + w_{\dot{m},rand}^2 \end{aligned} \quad (9)$$

Here, $w_{\dot{m}}^2$ is the uncertainty in mass flow rate, $w_{P_{atm,sys}}^2$ is the systematic uncertainty in atmospheric pressure, $w_{T_{atm,sys}}^2$ is the systematic uncertainty of the temperature, $w_{V_{n,sys}}^2$ is the systematic uncertainty in the velocity measured in the n^{th} section, $w_{x,sys}^2$ and $w_{y,sys}^2$ are the systematic uncertainties in the width and height, $w_{integration}^2$ is the uncertainty in the integration method, and $w_{\dot{m},rand}^2$ is the random uncertainty in the mass flow rate measurements.

The last step is to combine all the simplifications used in Appendix A. So, the complete uncertainty equation in uncertainty magnification factor (UMF) form can be seen in Equation 10.

$$\begin{aligned} \left(\frac{w_{\dot{m}}}{\dot{m}} \right)^2 &= (1)^2 \left(\frac{w_{P_{atm,sys}}}{P_{atm}} \right)^2 + (-1)^2 \left(\frac{w_{T_{atm,sys}}}{T_{atm}} \right)^2 + \left(\frac{V_1^2}{(\sum_{i=1}^n V_i)^2} \right) \left(\frac{w_{V_{1,sys}}}{V_1} \right)^2 + \dots \\ &\quad + \left(\frac{V_n^2}{(\sum_{i=1}^n V_i)^2} \right) \left(\frac{w_{V_{n,sys}}}{V_n} \right)^2 + (1)^2 \left(\frac{w_{x,sys}}{x} \right)^2 + (1)^2 \left(\frac{w_{y,sys}}{y} \right)^2 \\ &\quad + (1)^2 \left(\frac{w_{integration}}{\dot{m}} \right)^2 + (1)^2 \left(\frac{w_{\dot{m},rand}}{\dot{m}} \right)^2 \end{aligned} \quad (10)$$

This form of the uncertainty equation is much nicer- before each parameter's relative uncertainty is the UMF, which shows how much each parameter's relative uncertainty impacts the resultant's relative uncertainty.

Creating a preliminary uncertainty budget

The target uncertainty for this project is 15%, so to get an idea of how much uncertainty should be allotted per parameter, the team looked at the uncertainty for some different sensors that are likely to be used for the apparatus.

To measure atmospheric pressure, a pocket weather meter will be used. This sensor has an uncertainty of 3.133 psf, given that the average pressure at sea level on a standard day is 2117 psf, the relative uncertainty is about 0.148%. Since the experiment may not be operating under these exact conditions, the allotted uncertainty for pressure is rounded up to be 0.2%. Since the

pocket meter can measure values within the range expected with a small uncertainty, it is a reasonable sensor to use.

The pocket weather meter will also be used to measure temperature. This is partly for convenience as the same instrument can measure multiple measurands. The uncertainty in the temperature reading is $1.8 \text{ }^{\circ}\text{R}$, and with the average room temperature being about $531.67 \text{ }^{\circ}\text{R}$, this results in a relative uncertainty of 0.34%. To be safe, the uncertainty will be rounded up to 0.4%.

To measure the height and width of the test area, calipers will be used as they can accurately measure distances in the range the grid measurands are in. The calipers used have an uncertainty of 0.001116 inches, and for a measurement of about 5.664 inches (which is the proposed height and width of the testing area) this gives a relative uncertainty of 0.0197%. Again, the uncertainty is rounded up to 0.2% to be safe.

To determine how much uncertainty should be allotted for velocity, a bit more math is needed along with a few assumptions. First, the velocity sensor to be used has 2 different operating ranges, a low velocity range between 0–394 ft/min, and a high velocity range between 394–2953 ft/min. The systematic uncertainty of the tool changes when operating in the two different regions due to the accuracy of tool changing. These values are summarized in Table 1.

Table 1: Uncertainty table where V is the measured velocity in units of ft/min by the hot wire anemometer

Velocity Range	Systematic Uncertainty	Readability Uncertainty
0-394 ft/min	$(20 \text{ ft/min} + 0.05V)^2$	$(0.985)^2 \text{ ft/min}$
394-2953 ft/min	$(59.1 \text{ ft/min} + 0.05V)^2$	$(0.985)^2 \text{ ft/min}$

For the budget, the team considered two different cases: the case where all the velocities measured are in the low range, and the case where there is a mix of low and high velocities. The reason behind including two different cases is at low voltages the axial fan is expected to produce an average velocity in the lower velocity range. For higher voltages, the average velocity may be in the higher range, but due to the use of a duct there will also be low range velocities – more on this later in the section.

The uncertainty in the integration term can be calculated by Equation 11.

$$w_{\text{Integration}} = C(\Delta A)^2 \quad (11)$$

In each mass flow rate trial conducted, there will be 36 test points or 36 equal-sized areas. Comparing the error in integration for using 1 velocity measurement to 36 velocity measurements yields that the error in 36 measurements is 0.077% to that of the 1 measurement case. This was deemed small enough that there was not a need to increase the number of measurements any further. Since the value of the constant C is unknown, for the budget it is assumed that C does not cause the integration relative uncertainty to go above 4%.

The reason behind allotting 6% uncertainty to randomness is that it is a significant portion of the budget (see the UPC charts on page 14). So, providing a lot of room within the unpredictable section of air flow (as fluids often are) is a safe route to follow. This large uncertainty also considers the fact that there will only be a few trials conducted for each voltage, which will give a larger random uncertainty than if there were many trials at that voltage.

For the first case for velocity uncertainty: it is assumed that all speeds are in the lower region. It is also assumed the measured velocities are equal in each of the smaller areas. Substituting the relative uncertainties for the other parameters to see how much uncertainty can be allotted to velocity results in Equation 12,

$$(15\%)^2 = (1)^2(0.2\%)^2 + (-1)^2(0.4\%)^2 + \left(\frac{V}{36V}\right)^2 (w_{rel})^2 + \dots + \left(\frac{V}{36V}\right)^2 (w_{rel})^2 + (1)^2(0.2\%)^2 + (1)^2(0.2\%)^2 + (1)^2(4\%)^2 + (1)^2(6\%)^2 \quad (12)$$

This can be simplified to Equation 13 below.

$$(15\%)^2 = (0.2\%)^2 + (0.4\%)^2 + (0.2\%)^2 + (0.2\%)^2 + 36 \left(\frac{1}{36}\right)^2 (w_{rel})^2 + (4\%)^2 + (6\%)^2 \quad (13)$$

Solving this gives the initial relative uncertainty for velocity to be 78.9%. To give a little extra room with the uncertainty budget, the relative uncertainty is rounded down to 78%. This value is quite high and intuitively seems like it would not be valid; however, since the UMF of the velocity terms is so small the relative uncertainty in velocity can be quite large while keeping a small uncertainty in the resultant mass flow rate.

The next step is to determine the range of acceptable velocities for the low velocity range. Relative uncertainty for any parameter (k) is defined in Equation 14.

$$\frac{w_k}{k} = w_{rel} \quad (14)$$

Plugging in the equation for systematic uncertainty for low range velocities and the 78% for relative uncertainty into Equation 14 yields Equation 15.

$$\frac{\sqrt{(20 + 0.05V)^2 + (0.985)^2}}{V} \leq 78\% \quad (15)$$

Which gives a minimum velocity of 27.4 ft/min for the ‘all lower speeds’ case. The maximum velocity for the all low-speed condition is 394 ft/min which is induced by the limitation of the sensor.

The second case to consider is if there is a mix of low- and high-end velocities. Given the geometry of the fan, it is expected that there will be slower flow in the shaded areas of Figure 4.

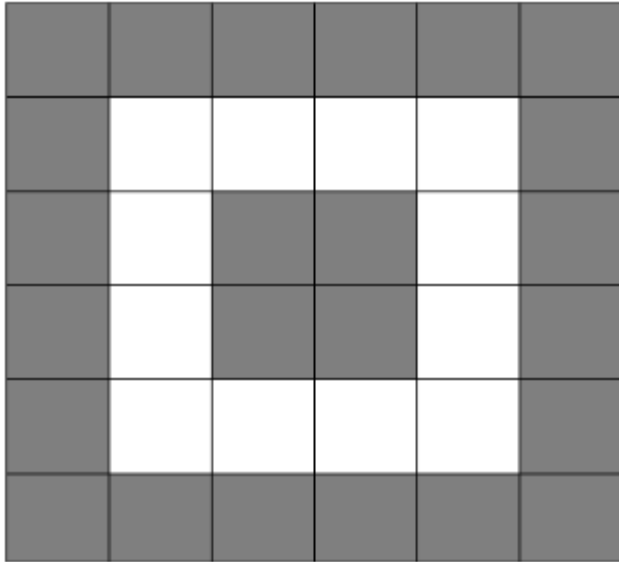


Figure 4: A 6x6 testing area divided up into equal area slices with low velocity sections in dark gray and high velocity sections in white.

This leads to 24 slower speed and 12 higher speed sections. The reasoning behind these locations of slower speeds is due to a couple different reasons. First, the fan is forcibly moving air causing the flow to be turbulent, which causes vortices within the flow. Secondly, due to the use of a duct there is an induced ‘no-slip condition’ which means that the flow along the surface of the duct will have 0 velocity.

With the introduction of two different ranges of speeds the uncertainty equation becomes a bit more complex. Within these two ranges, it is assumed that all low-speed sections will have the same relative uncertainty, while the high-speed sections will have the same relative uncertainty but different from the low-speed sections. This assumption allows Equation 10 to simplify down to Equation 16.

$$(15\%)^2 = (0.2\%)^2 + (0.4\%)^2 + (0.2\%)^2 + (0.2\%)^2 + \frac{1}{24} (w_{rel,low})^2 + \frac{1}{12} (w_{rel,high})^2 + (4\%)^2 + (6\%)^2 \quad (16)$$

Since the minimum velocity for the higher range is 394 ft/min, that value can be used to solve for the higher range’s maximum relative uncertainty using Equation 17 and the systematic uncertainty for high range velocities.

$$\frac{\sqrt{(59.1 + 0.05(394))^2 + (0.985)^2}}{394} \leq w_{rel,high} \quad (17)$$

This gives a higher speed relative uncertainty of 20%. Plugging this back into Equation 16 results in Equation 18.

$$(15\%)^2 = (0.2\%)^2 + (0.4\%)^2 + (0.2\%)^2 + (0.2\%)^2 + \frac{1}{24} (w_{rel,low})^2 + \frac{1}{12} (20\%)^2 + (4\%)^2 + (6\%)^2 \quad (18)$$

Solving Equation 18 yields a relative uncertainty for the lower speeds of 57.8%, where again this will be rounded down to 57%.

Similar to how it was done for the low velocity case, by using Equation 19, the minimum low-end velocity can be solved for below.

$$\frac{\sqrt{(20 + 0.05V)^2 + (0.985)^2}}{V} \leq 57\% \quad (19)$$

This equation yields a minimum velocity for the low-speed velocities of 38.5 ft/min.

To summarize, if the measured velocities are all within the low-speed range it must be above 27.4 ft/min, and if the measured velocities are a mix between high and low-speed ranges it must be above 38.5 ft/min to meet the uncertainty goal.

All relative uncertainty values for each parameter can be found in Table 2 below. As a reminder, there are two different velocity profiles: the low speed only profile and the mix of high and low speed profiles. The uncertainties are labeled accordingly in the below table.

Table 2: Relative uncertainty allocated for each parameter

Parameter	Relative Uncertainty
Pressure	0.2%
Temperature	0.4%
Length	0.2%
Width	0.2%
Velocity (low speeds case)	78%
Velocity (mixed speeds case)	Low velocities: 57% High velocities: 20%
Integration scheme	4%
Random	6%

In terms of the uncertainty budget, each parameters contribution for each case can be seen below in the following charts through their uncertainty percent contribution (UPC). Figure 5 shows the UPC pie-chart for the condition of just low speeds for velocity (0–394 ft/min range). Figure 6

shows the UPC pie-chart for the condition of mixed speeds for velocity (0–394 ft/min for low speeds and 394–2953 ft/min for high speeds). Random uncertainty takes up most of the chart followed by the integration uncertainty in both cases. This is due to the UMF terms for both integration and random uncertainty terms being 1 so there is no reduction in the scaling on the these uncertainties for the mass flow rate.

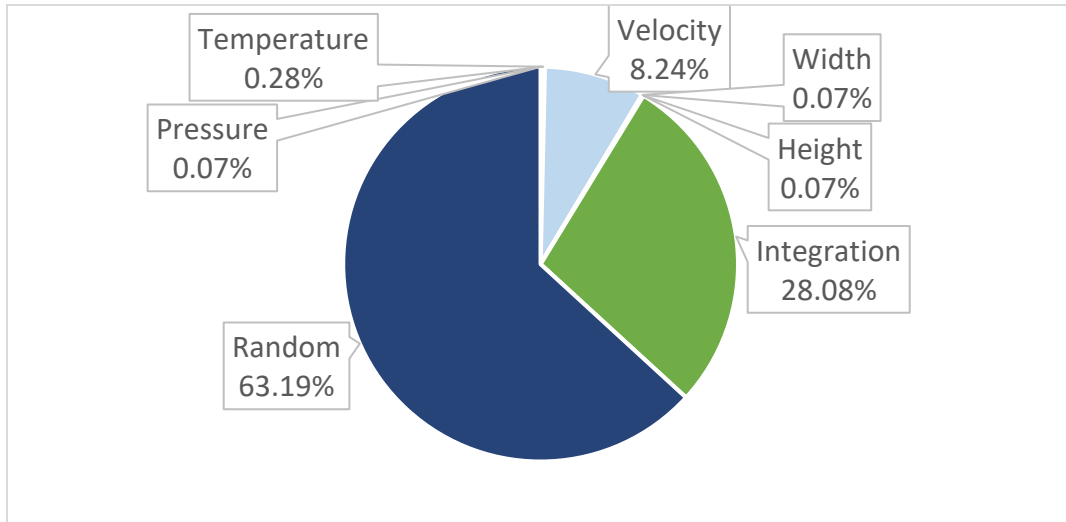


Figure 5: UPC chart for each parameter in the low-speed range condition

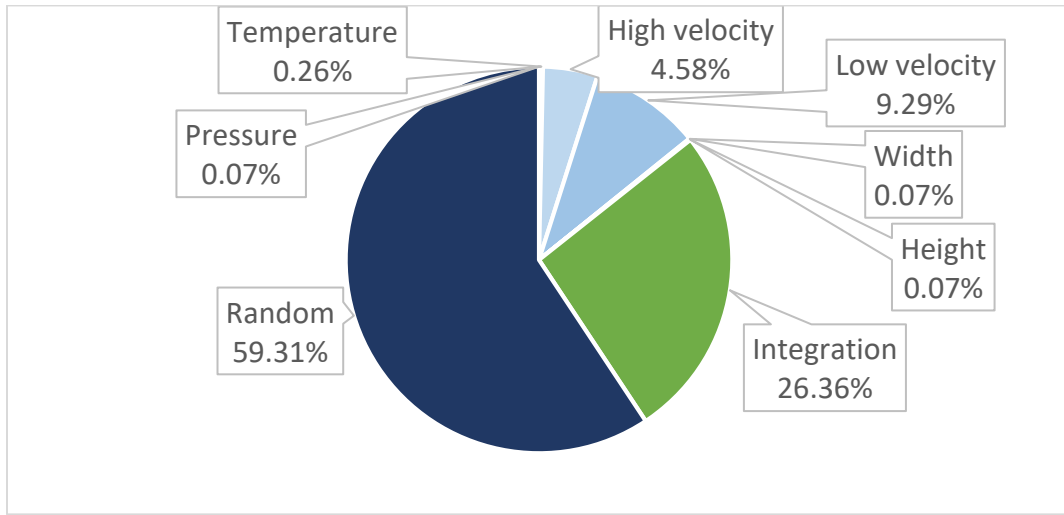


Figure 6: UPC chart for each parameter in the mixed speed range condition

Apparatus, Procedure, and Design Space Plot

One goal in the overall experiment is to maximize the accuracy and precision with which the anemometer can be placed in each square measurement grid. The motivation for this is to minimize the relative uncertainty allocated to random uncertainty and make it easier to gather multiple trials worth of data. An infographic for the proposed apparatus can be found in Figure 7.

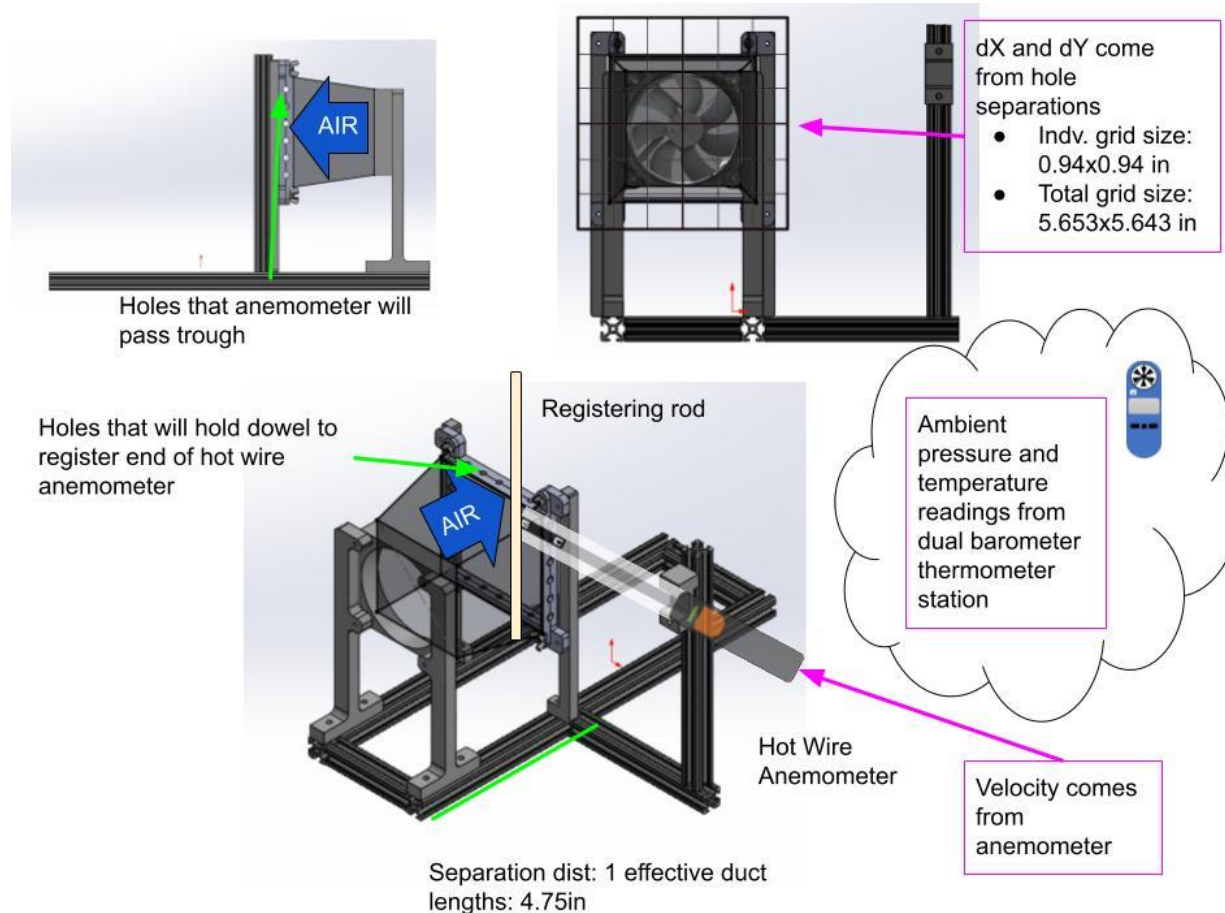


Figure 7: Proposed testing apparatus for mass flowrate experiment

The experimental apparatus has a jig that has two sets of holes perpendicular to each other. The purpose of one set of holes is to allow a registering rod through, while the other set guides the anemometer through. Where these holes intersect is where the measurement will take place. An 80/20 (extruded aluminum slot/rail system) frame is used to keep all devices level and make the data gathering process more efficient. A duct contains the flow and is attached to the fan and the alignment jig. A dual thermometer barometer is used to measure the atmospheric temperature and pressure in the room. These values are needed to calculate the local density of the atmosphere. A set of calipers will be used to measure the distances between each grid measurement to ensure that the experiment remains properly aligned. Finally, although it is not used in the DRE, a digital multimeter will be used to measure the voltage being supplied to the

fan. This voltage value is needed when generating the final plot showing the mass flow rates at different voltage inputs.

The specifications for each sensor are tabulated in Table 3. Dial calipers do not have a specified accuracy, so the value assigned to resolution was used for the readability uncertainty and the accuracy uncertainty. Table 3 also contains the resolution and readability for the digital multimeter that will be used as a voltmeter in the apparatus. The voltage measurand does not appear in the DRE nor the uncertainty calculations, but when finding the uncertainty in the fan curve these values will be needed.

Table 3: Measurand Table with measuring tool name and uncertainty values for resolution and accuracy

Measurand	Symbol	Readout Units	Tool	Resolution	Accuracy
Atmospheric Pressure	P_{atm}	hPa	Kestral 3500 NV	$\pm 0.1 \text{ hPa}$	$\pm 1.5 \text{ hPa}$
Atmospheric Temperature	T_{atm}	°F	Kestral 3500 NV	$\pm 0.1^\circ\text{F}$	$\pm 1.8^\circ\text{F}$
Height	y	Inches	Dial Calipers	$\pm 0.001 \text{ in}$	----
Width	x	Inches	Dial Calipers	$\pm 0.001 \text{ in}$	----
Velocity	V	Feet per Minute	Testo 405i	$\pm 1 \text{ fpm}$	$\pm(20 + 5\% \text{ m. v.})$ $\pm(59 + 5\% \text{ m. v.})$
Voltage	V_{elec}	Volts	Milwaukee DMM	$\pm(0.001V)$ $\pm(0.01V)$	$\pm(0.5\% \text{ m. v.} + 2 \text{ dgt})$

A summary of the minimum and maximum sensor specifications are shown in Table 4. To simplify things a bit, the measurands of width and height were combined into one term: distance. Using the definition of relative uncertainty, and the relative uncertainties that were calculated for each measurand in Table 2, absolute minimums were then calculated. Given the tools specified operating range and laboratory conditions, practical maximums and minimums were selected.

Table 4: Minimum and maximum values for each type of measurand

Measurand	Uncertainty Calculated Minimum	Measurand Maximum	Practical Minimum	Practical Maximum
Temperature [R]	450	720	527.67	537.67
Pressure [psf]	1570	2297	2050	2150
Distance [in]	2.5	6	4.72	6
Velocity [fpm] (Low flow speeds)	27.4	394	27.4	394
Velocity [fpm] (Low flow speeds with high speeds)	38.5	394	38.5	394
Velocity [fpm] (High flow speeds)	394	2953	394	2953

The apparatus was designed with input from existing experimental setups like the one shown in Figure 8. Some of the setups use ducts, flow straighteners, or a combination of both. The use of a duct is common, as air conditioning ducts are a major commercial use of volumetric flow measurement. The flow straighteners are used to minimize the amounts of points needed to measure as they produce a uniform velocity profile. A flow straightener would block too much of the flow and contribute excessive losses; however, a duct can be employed if the losses in mass flow are negligible. With a duct length of one effective fan diameter the best of both worlds is achieved. The flow is contained inside a duct, allowing for a complete velocity profile to be gathered. Without a duct, some ambient air is drawn through and past the grid, increasing the mass flow measured. The duct is also short enough to prevent excessive losses. To validate this claim that the duct is short enough to prevent noticeable losses, two tests at 5V were run on the refined apparatus. The first trial was run with no duct and produced a mass flow rate of $0.1497 \frac{\text{slug}}{\text{min}}$. The second trial was run with a duct and produced a mass flow rate of $0.1455 \frac{\text{slug}}{\text{min}}$. The percentage difference between the results of both trials was approximately 3%. With this small difference, the team was confident that the duct would only positively impact the experiment by reducing the large influx of ambient air at the higher fan voltages. For more information on this testing please see Appendix B.

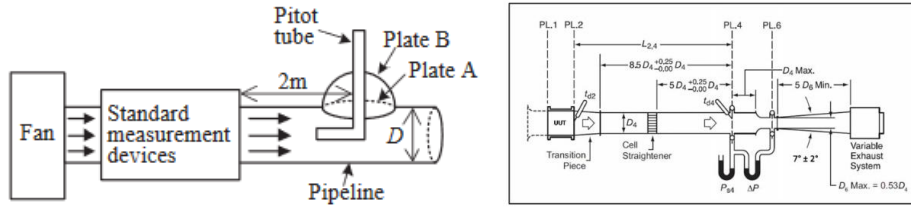


Figure 8: Other test apparatuses suggested by standards and research papers

To accommodate the duct and larger flow grid, the apparatus is raised off the ground. To ensure that the velocity profile is captured as accurately as possible, 36 points are used for the grid. This ensures that any irregularities in the flow are accounted for.

The remaining challenge is dimensioning the distances in the apparatus. For the distance from the outlet of the fan to the measurement jig, the effective duct length equation is used. The effective duct length states that for low RPM flows, which this fan is, the distance is 2.5 times the diameter. This will allow no negative flow velocities to be present and a slightly more uniform velocity profile to integrate. Figure 9 details how the flow transforms over the effective duct length. However, to mitigate mass flow losses, a duct with a length of the fan diameter, 120mm, is used. As a result, the velocity profile is not entirely uniform, however with the density of the grid, the flow irregularities can be accurately captured.

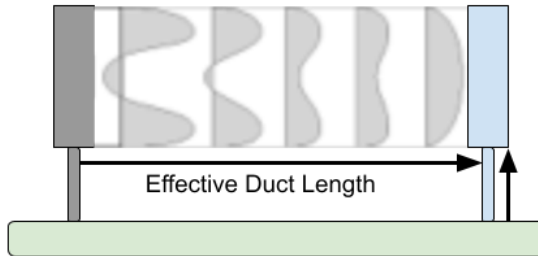


Figure 9: Effective duct length diagram

The height off the ground of the apparatus was determined once the apparatus was constructed. The requirement is that the fan and the grid are aligned at their centers. The grid being swept by the anemometer is larger than the fan area. This is to take more data points, and capture more of the velocity field. This large area allows the flow blockage caused by the apparatus and anemometer to be of less concern.

The procedure of gathering the measurements will follow a grid column-row approach. A visual representation of this can be found in Figure 10. Each grid in a column will have its center flow velocity measured 10 times and then the process will shift down a row and the process will repeat until the entire area of the grid has been measured.

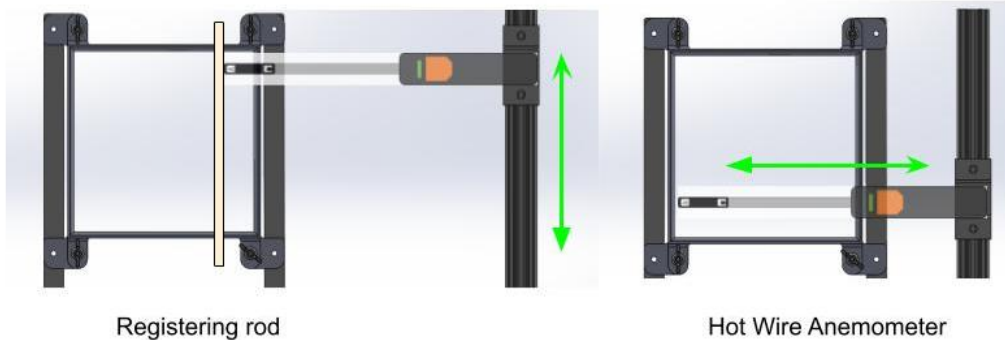


Figure 10: Experimental procedure visualization

The apparatus ensures that the fan always remains centered in the flow grid, and that the anemometer remains aligned in the flow grid. The anemometer is simple to use with the downloadable app. The experiment developed by the team uses 10 values from the anemometer that are then averaged to form 1 data point with the readability as the standard deviation.

The measurement scheme depicted in Figure 10 above is repeated a total of 3 trials at each voltage level to reduce random uncertainty. The voltage levels used during this experiment were 3V, 5V, 10V and 12V.

After all data has been recorded the values are read into the MATLAB post-processing script where the values for mass flow rate and total uncertainty are calculated.

To visualize that the uncertainty is allocated properly, and the proper tools were selected to perform the experiment to within the goal of 15% uncertainty in mass flowrate, a design space plot was created. The design space plot for the experiment is in Figure 11. Using the main DRE found in Equation 8, the x-axis and y-axis were separated into variables that could be controlled on the x-axis, and variables that could not be controlled on the y-axis. These broken-down equations are shown by Equation 20 and Equation 21 respectively. Using these equations for the axis results in the slope of a line on the plot is equal to the mass flowrate.

$$X_{axis} = \frac{n}{(x)(y)} \quad (20)$$

$$Y_{axis} = \frac{P_{atm} \sum_{i=1}^n V_i}{R T_{atm}} \quad (21)$$

Assuming the use of 36 points of measurements, the red vertical line is created by taking n , the number of measurement points, divided by the overall test area of 5.664 inches by 5.664 inches. The red vertical line will intercept the sloped blue lines which are an estimate of the low and high mass flow rate of the fan. These values were calculated by multiplying the lowest and highest average volumetric flow rates, given by the specification sheet of the fan, by the density of air. Density of air is estimated using a temperature of 72 °F and a pressure of 992.4 hPa, which was recorded in the proposed lab space. The minimum expected mass flow rate is 0.0940 slugs/min and the maximum expected mass flow rate is 0.2305 slugs/min

To prove that the intersection points are reasonable, and the experiment can be performed, lower and upper bounds for the y-axis need to be implemented. Using Equation 21, the equations to find the minimum and maximum allowable y-values are found in Equation 22 and 23 respectively.

$$Y_{axis,min} = \frac{P_{atm,min} V_{sum,min}}{R T_{atm,max}} \quad (22)$$

$$Y_{axis,max} = \frac{P_{atm,max} V_{sum,max}}{R T_{atm,min}} \quad (23)$$

The summation of velocity can be estimated by using Equation 24. Using this estimation, Equations 22 and 23 can be simplified so only one value for velocity is needed to calculate the lower bound and another to calculate the upper bound.

$$\sum_{i=1}^n V_i \approx (V_{avg})(n) \quad (24)$$

The larger allowed average low velocity was calculated to be 38.5 fpm in the mixed velocity condition. This value will be used to calculate the lower y-axis bound because it is higher than the other calculated value of 27.4 fpm. If the experiment can work with 38.5 fpm, then it will work for the lower average velocity. An estimated value for the y-axis lower bound can be found with Equation 25.

$$Y_{axis,min} = \frac{P_{atm,min} (V_{avg,min} n)}{R T_{atm,max}} = 3.0777 \frac{\text{slug}}{\text{ft}^2 \text{ min}} \quad (25)$$

The upper y-axis bound is governed by an average velocity is 2953 fpm, which is the maximum velocity the sensor can measure. The fan is not expected to reach this speed, but it is set as the practical maximum for the experiment due to the sensor. The y-axis upper bound can be estimated using Equation 26 below.

$$Y_{axis,max} = \frac{P_{atm,max} (V_{avg,max} n)}{R T_{atm,min}} = 252.2735 \frac{\text{slug}}{\text{ft}^2 \text{ min}} \quad (26)$$

These horizontal bounds are represented on Figure 11 by black lines, with the minimum being a solid black line and the maximum being a dashed black line. The upper y-axis bound is outside of the view of the plot and does not play a role in analyzing if the experiment if possible since it is so high up.

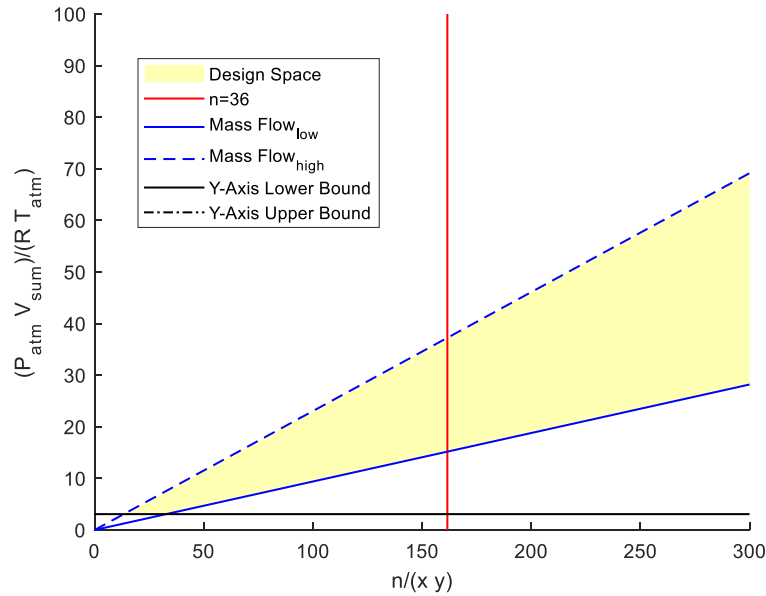


Figure 11: Mass flowrate design space plot with inverse equal area on the x-axis and density of air multiplied by the sum of velocity on the y-axis.

It is easy to see that the intersections of the red vertical line with the sloped blue lines are within the black horizontal lines, proving that the experiment is possible and a goal of 15% uncertainty in mass flowrate is attainable under these assumptions.

Data and Analysis

Using the procedure outlined in the Apparatus, Procedure, and Design Space Plot section of the report, data for individual trials were collected. Representative data for the first trial of the 5V testing is shown below as the post processing procedure is outlined. The representative values for the voltage (V_{elec}), atmospheric pressure (P_{atm}) and temperature (T_{atm}), overall width of the flow grid (x), and overall height of the flow grid (y) are shown in Table 5.

Table 5: Representative Environment Values for 5.258V Trial

Parameter	Representative Value	Units
Voltage	5.258	V
Atmospheric Temperature	534.3	°R
Atmospheric Pressure	2103.8	psf
Width	0.471	ft
Height	0.470	ft

Representative values for velocity at the different flow grid measurement locations are represented in Figure 12 which is a 3D plot of the flow field. To get a velocity for one point, ten velocities were taken at a single location and an average was taken to represent the velocity for that location. Standard deviation of the ten velocity values was also calculated for the purpose of uncertainty calculations for velocity. This process was repeated for all 36 data collection points.

Calibration of the Testo hotwire anemometer was required and a correction factor of 1.046 was found and used to correct the values of velocities by multiplying the average velocity and the standard deviation by the correction factor. Information on how the correction factor was calculated can be found in Appendix D. The adjusted velocity values are the velocity values present in Figure 12, to see the unprocessed data tables please see Appendix E.

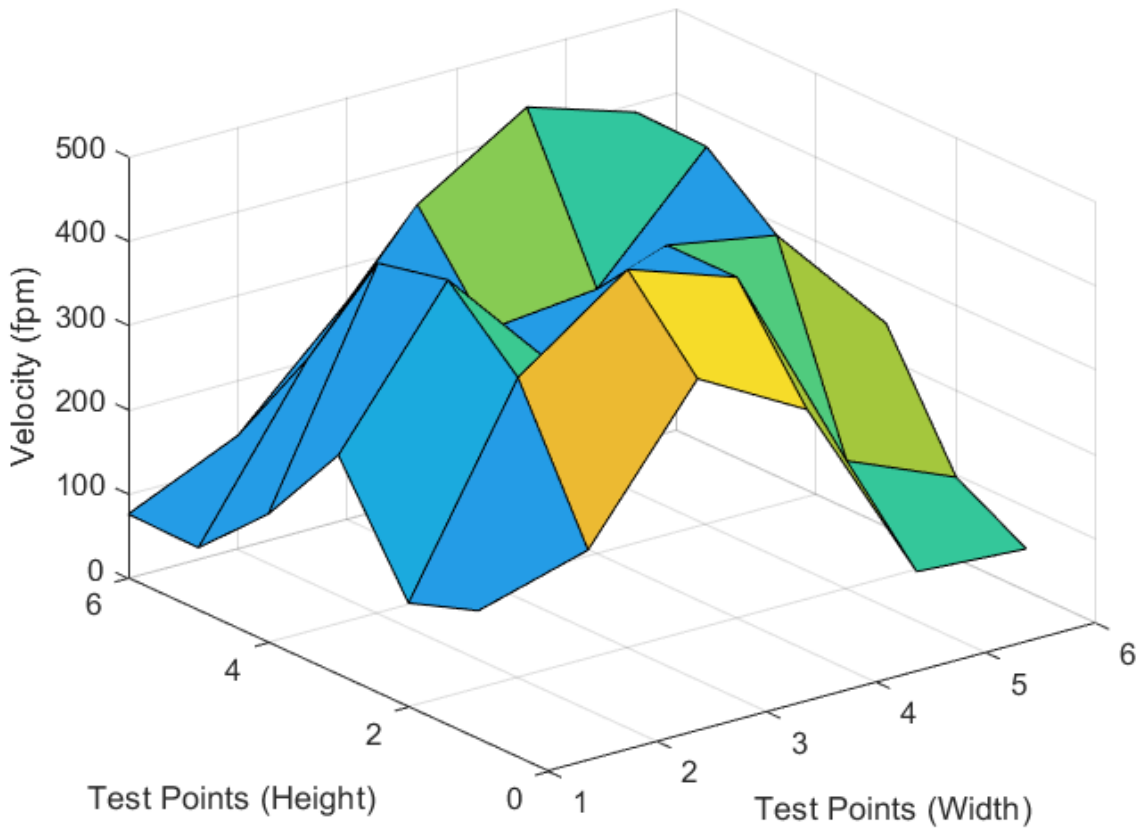


Figure 12: Representation of corrected velocity measurements for 5.258V Trial at all 36 measurement points

Using the DRE equation from Equation 8 the mass flow rate for this trial was calculated to be 0.134 slugs/min. The error for the individual mass flow trial is composed of the systematic errors of the measurands and the uncertainty due to the integration error. The equations for calculating systematic error are outlined in Appendix A and the process of how to calculate the integration error is outlined in Appendix C.

Table 6 is an Uncertainty Table for one complete 5V trial, specifically the 5.258V trial, of the experiment to determine the mass flow rate of an axial fan. The first two rows represent the environmental data, Atmospheric Pressure (P_{atm}) and Temperature (T_{atm}) used to calculate the density of air. The third and fourth rows are the width (x) and height (y) of the flow grid respectively. The remaining rows in the table are the corrected velocity measurement in each sub grid, uncertainty due to integration, and the resulting mass flow rate for the trial. Values in the columns from **Error! Not a valid bookmark self-reference.** were calculated using the uncertainty equations discussed in the Modeling section of the report. The resultant mass flow rate for this 5-volt trial was calculated using Equation 8. For more details on the equations used to calculate the systematic uncertainties for all parameters and the UMF terms for velocity refer to Appendix A.

Table 6: Uncertainty Table for 5.258V Trial for the 5V setting group

Parameter	Representative Value	Syst. Uncertainty	Units	Relative Uncertainty (%)	UMF	RSSC (%)	UPC (%)
Atmospheric Temperature	534.3	1.801	R	0.337	1.000	0.337	0.506
Atmospheric Pressure	2103.8	3.135	psf	0.149	1.000	0.149	0.099
Width	0.471	9.317E-05	ft	0.020	1.000	0.020	0.002
Height	0.470	9.317E-05	ft	0.020	1.000	0.020	0.002
Velocity 1	153	48.056	fpm	31.487	0.016	0.508	1.150
Velocity 2	189	50.136	fpm	26.481	0.020	0.530	1.251
Velocity 3	357	59.490	fpm	16.648	0.038	0.629	1.762
Velocity 4	286	53.843	fpm	18.855	0.030	0.569	1.443
Velocity 5	58	23.481	fpm	40.283	0.006	0.248	0.274
Velocity 6	50	22.853	fpm	45.516	0.005	0.242	0.260
Velocity 7	124	91.329	fpm	73.937	0.013	0.965	4.152
Velocity 8	356	67.933	fpm	19.097	0.038	0.718	2.297
Velocity 9	449	85.423	fpm	19.032	0.047	0.903	3.632
Velocity 10	404	104.900	fpm	25.944	0.043	1.109	5.478
Velocity 11	152	51.616	fpm	34.053	0.016	0.546	1.326
Velocity 12	97	38.175	fpm	39.359	0.010	0.404	0.725
Velocity 13	261	91.552	fpm	35.125	0.028	0.968	4.172
Velocity 14	433	105.653	fpm	24.382	0.046	1.117	5.557
Velocity 15	294	51.250	fpm	17.448	0.031	0.542	1.308
Velocity 16	404	90.213	fpm	22.323	0.043	0.954	4.051
Velocity 17	381	83.306	fpm	21.874	0.040	0.881	3.455
Velocity 18	241	85.880	fpm	35.613	0.025	0.908	3.671
Velocity 19	153	64.462	fpm	42.237	0.016	0.681	2.069
Velocity 20	415	90.830	fpm	21.883	0.044	0.960	4.107
Velocity 21	301	65.291	fpm	21.715	0.032	0.690	2.122
Velocity 22	314	73.633	fpm	23.458	0.033	0.778	2.699
Velocity 23	448	140.854	fpm	31.469	0.047	1.489	9.876
Velocity 24	232	86.892	fpm	37.389	0.025	0.918	3.759
Velocity 25	74	27.391	fpm	36.788	0.008	0.290	0.373
Velocity 26	264	74.163	fpm	28.135	0.028	0.784	2.738
Velocity 27	411	91.859	fpm	22.346	0.043	0.971	4.200
Velocity 28	492	84.518	fpm	17.192	0.052	0.893	3.556
Velocity 29	450	95.655	fpm	21.245	0.048	1.011	4.555
Velocity 30	194	61.092	fpm	31.462	0.021	0.646	1.858
Velocity 31	76	28.515	fpm	37.391	0.008	0.301	0.405
Velocity 32	134	68.641	fpm	51.122	0.014	0.726	2.345
Velocity 33	258	55.131	fpm	21.347	0.027	0.583	1.513
Velocity 34	214	77.615	fpm	36.293	0.023	0.820	2.999
Velocity 35	168	64.263	fpm	38.203	0.018	0.679	2.056
Velocity 36	174	63.624	fpm	36.542	0.018	0.673	2.015
Integration	-	2.699E-04	slugs/min	0.202	1.000	0.202	0.182
Mass Flowrate	0.134	0.006	slugs/min	-	-	4.738	100

This process is repeated two more times to calculate an average mass flow rate for a specified setting of the axial fan. The equation to find the average mass flow rate and the uncertainty are presented below in Equation 27 and Equation 28 respectively.

$$\dot{m}_{avg} = \frac{1}{n} \sum_{i=1}^n \dot{m}_i \quad (27)$$

$$w_{\dot{m}_{avg}}^2 = \left(\frac{\dot{m}_1}{\sum_{i=1}^n \dot{m}_i} \right)^2 (w_{\dot{m}_1})^2 + \left(\frac{\dot{m}_2}{\sum_{i=1}^n \dot{m}_i} \right)^2 (w_{\dot{m}_2})^2 + \left(\frac{\dot{m}_3}{\sum_{i=1}^n \dot{m}_i} \right)^2 (w_{\dot{m}_3})^2 + w_{rand}^2 \quad (28)$$

The random uncertainty is calculated using Equation 29 below.

$$w_{rand} = \frac{(t)(S_{\dot{m}})}{\sqrt{n}} \quad (29)$$

Where n is the number of trials being averaged, $S_{\dot{m}}$ is the standard deviation of the different trials, and t is a value selected from the T-Statistic Table with 95% confidence. For the purposes of this experiment, the t value will be 4.303 since there were only three trials performed for each voltage group, which allows for two degrees of freedom.

A sample Uncertainty Table for the 5V group of measurements is shown in Table 7. Random uncertainty contributed the most to the uncertainty of the average- making up over 50% of the overall uncertainty.

Table 7: Uncertainty Table for the 5V group of mass flow measurements resulting in an average of 0.129 slugs/min for 5V setting

Parameter	Representative Value	Syst. Uncertainty	Units	Relative Uncertainty (%)	UMF	RSSC (%)	UPC (%)
Mass Flow 1	0.134	0.006	slugs/min	4.738	0.346	1.637	19.287
Mass Flow 2	0.125	0.005	slugs/min	4.004	0.325	1.300	12.157
Mass Flow 3	0.127	0.006	slugs/min	4.513	0.330	1.489	15.952
Random	-	0.010	slugs/min	2.703	1.000	2.703	52.603
Avg. Mass Flowrate	0.129	0.005	slugs/min	-	-	3.727	100

The process of collecting and processing the data and uncertainty was repeated for the 3V, 10V, and 12V groups, and the mass flow data can be found in Appendix F. Figure 13 shows all the data collected from the different trials on a mass flow rate versus voltage graph.

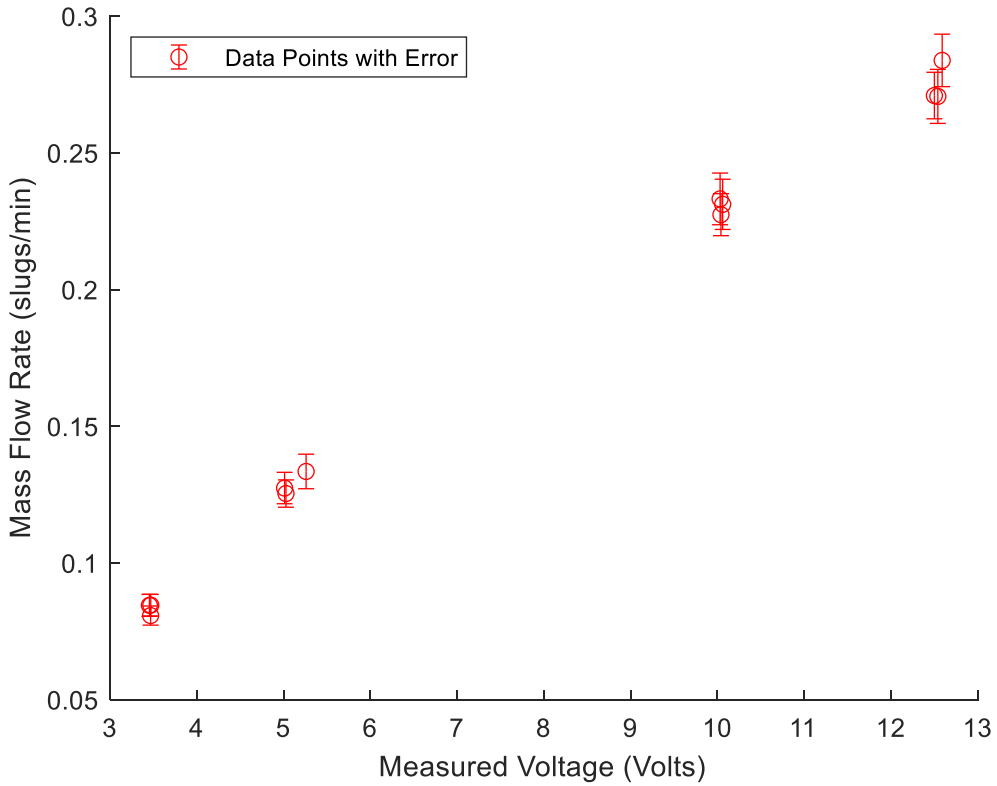


Figure 13: Plot of calculated mass flow rate against measured voltage

The data shows a relatively linear trend, so linear regression will be used to analyze the relationship between mass flow rate of the fan and the voltage input to the fan. A linear regression can be made using the least squares method with matrices and vectors as shown in Equation 30.

$$[A]\{\vec{x}\} = \{\vec{b}\} \quad (30)$$

Where $[A]$ is the coefficient matrix made of regressors, $\{\vec{x}\}$ is the parameter vector, and $\{\vec{b}\}$ is the regressand vector filled with the values the linear fit is being made for. To get an estimate for the slope and intercept of a sloped line the normal equation is used as shown in Equation 31.

$$\{\vec{x}\} = ([A]^T [A])^{-1} ([A]^T \{\vec{b}\}) \quad (31)$$

The linear regression will still have some uncertainty associated with the slope and intercept values it produces. Uncertainty for the slope of the linear regression is calculated using Equation 32.

$$w_m^2 = \frac{\sum (y_i - \bar{y})^2}{(\sum (x_i - \bar{x})^2)^2} w_x^2 + \frac{1}{\sum (x_i - \bar{x})^2} w_y^2 \quad (32)$$

Where \bar{x} and \bar{y} are the averages of the data values for the horizontal axis (voltage) and vertical axis (mass flow rate) respectively, w_x is the average systematic uncertainty for the horizontal axis variable (voltage), and w_y is characterized by Equation 33 below.

$$w_y^2 = w_{y,sys}^2 + \left(2 \left(\frac{\sum (y_i - (mx_i + b)^2)}{n - 2} \right)^{\frac{1}{2}} \right)^2 \quad (33)$$

Where n is the number of data points, and $w_{y,sys}$ is the average systematic uncertainty for the vertical axis variable.

All the post processing mentioned in this section is completed by the MATLAB script shown in Appendix G for reference.

Results and Discussion

The overall results of the experiment are shown in Table 8 with the average mass flow rate for the 3V, 5V, 10V, and 12V averaged voltage settings. All calculated mass flows have a relative uncertainty below 4% which is well below the target of 15%. While the fan specifies 3V as the minimum voltage, the fan drew 3.45V at the minimum setting. The same behavior was found at the opposite end with the fan drawing a maximum of 12.54V for the 12V expected setting.

Table 8: Average mass flowrates for average voltages of the different trial groups

Average Voltage of Trials (V)	Average Mass Flow Rate (slugs/min)	Uncertainty (slugs/min)	Relative Uncertainty (%)
3.462	0.083	0.003	3.424%
5.098	0.129	0.005	3.727%
10.04	0.231	0.006	2.443%
12.54	0.275	0.008	2.991%

All the different mass flow rate trials with their associated voltage setting and uncertainty are shown in Table 9. These are the values that will be used to make a proper linear regression of the data and show the relationship between mass flow rate and voltage. The regression of the experimental data is directly compared to the regression of expected operating volumetric flow rate of the fan. Using the average density of air from all the experimental trials (0.0022855 slug/ft³), the volumetric flow is converted to a mass flow rate. This conversion is recorded in Table 10.

Table 9: All calculated mass flow rates with corresponding voltage and uncertainty

Measured Voltage (V)	Uncertainty in Voltage (V)	Calculated Mass Flow Rate (slug/min)	Uncertainty in Mass Flow Rate (slug/min)
3.452	0.019	0.085	0.004
3.466	0.019	0.081	0.003
3.468	0.019	0.085	0.004
5.258	0.028	0.134	0.006
5.026	0.027	0.125	0.005
5.010	0.027	0.127	0.006
10.03	0.07	0.233	0.009
10.04	0.07	0.227	0.008
10.06	0.07	0.231	0.009
12.54	0.08	0.271	0.010
12.59	0.08	0.284	0.010
12.5	0.08	0.271	0.009

Table 10: Expected volumetric flow rates for different voltage settings for the Wathai axial fan

Voltage (V)	Expected Volumetric Flow Rate (CFM)	Converted Mass Flow Rate (slugs/min)	10% Uncertainty (slugs/min)
3	46.0	0.105	0.011
5	56.8	0.130	0.013
10	85.0	0.194	0.019
12	92.3	0.211	0.021

The experimental data and expected data are plotted on a mass flow rate versus measured voltage graph as depicted in Figure 14. The vertical error bars for the experimental data are the uncertainty of the mass flow rate for that individual trial, for reference those uncertainty values are in Table 9. The vertical error bars for the expected data are a 10% uncertainty calculated from the converted mass flow value since the fan reports a 10% uncertainty for the volumetric flow rate.

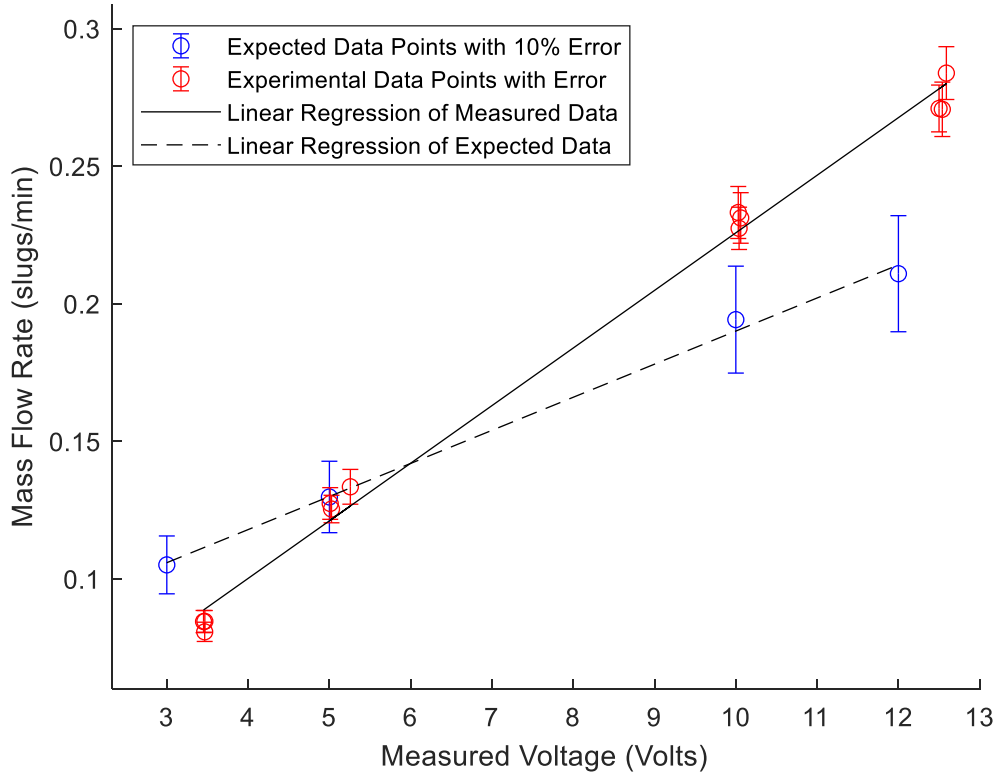


Figure 14: Comparison of linear regression of experimental data and expected data for the mass flow rate of Wathai axial fan at different voltage settings

The experimental data shows that the fan was underperforming compared to expected values in the 3V region and over performing compared to expected values in the 12V region. The linear regression for the experimental data is characterized by Equation 34 and the linear regression for the expected data is characterized by Equation 35.

$$\dot{m}_{experiment} = 0.0209 \pm 0.0012 \frac{slugs}{(min)(Volts)} (V_{elec}) + 0.0164 \frac{slugs}{min} \quad (34)$$

$$\dot{m}_{expected} = 0.0120 \frac{slugs}{(min)(Volts)} (V_{elec}) + 0.0699 \frac{slugs}{min} \quad (35)$$

To draw conclusions from this comparison an additional table was made to compare the expected and experimental data gathered. The results of this are shown in Table 11. The calculated mass flow rate was converted to volumetric flow rate by dividing the mass flow rate for a specific trial by the density of air calculated for that trial. The 5V trials had the smallest percent error and percent difference values of 1.36% and 1.37% respectively. The 12V trials had the largest percent error and percent difference at 35.91% and 30.44% respectively. The values calculated for the 3V and 10V trials and percent errors and percent differences ranging from the upper teens to the mid-twenties.

Table 11: Percent error and percent difference Calculations to compare the expected and experimental data

Measured Voltage (V)	Calculated Mass Flow Rate (slugs/min)	Calculated Volumetric Flow Rate (CFM)	Expected Voltage (V)	Expected Volumetric Flow Rate (CFM)	Percent Error (%)	Percent Difference (%)
3.452	0.085	36.7	3	46	20.12	22.37
3.466	0.081	35.6	3	46	22.52	25.38
3.468	0.085	37.0	3	46	19.63	21.77
5.258	0.134	58.2	5	56.8	2.49	2.46
5.026	0.125	54.9	5	56.8	3.42	3.48
5.01	0.127	56.0	5	56.8	1.36	1.37
10.03	0.233	101.2	10	85	19.03	17.38
10.04	0.227	99.6	10	85	17.21	15.85
10.06	0.231	101.7	10	85	19.61	17.86
12.54	0.271	117.5	12	92.3	27.34	24.05
12.59	0.284	125.4	12	92.3	35.91	30.44
12.5	0.271	118.5	12	92.3	28.37	24.85

Conclusion

In this paper, the mass flow rate through an electronic axial computer fan was studied through the development of an experiment. The mass flow rate of the fan was experimentally determined at the 3V, 5V, 10V, and 12V levels with average mass flow rates of 0.083, 0.1129, 0.231, and $0.275 \frac{\text{slug}}{\text{min}}$ respectively. The target uncertainty for the experiment was $\pm 15\%$. This target was met for each voltage level with uncertainties of 3.425, 3.725, 2.442, and 2.992 percent respectively.

The experiment successfully met the uncertainty target because of the choice of sensors, the number of points sampled during each trial, and the number of trials taken. The grid used in this experiment included 36 points which reduced the integration error substantially and accounted for more variation in the velocity flow field.

The percent difference from the manufacturer's published values cannot be overlooked as some trials had larger deviations. For the 3V, 5V, 10V, and 12V trials the averaged percent difference to the manufacturer-published flow rates were 23.17, 2.44, 17.03, and 26.45 percent. Although some of these percent differences are large, the team is confident in the results and the uncertainty. In the future, further experiments should analyze the power and RPM of the fan to confirm the credibility of the manufacturer spec sheet, as those are the other reported values at each voltage level. Determining the credibility of the manufacturer's specifications will confirm or dispute the accuracy of the fan profile the team generated.

While developing the experiment, the team learned that quick testing while designing an experiment is essential. Sometimes to test a theory simple cardboard and handheld pitot tubes will more than suffice. Spending hours designing a 3D-printed duct or large-scale test rig to test if an assumption is valid is not necessary. The time instead should be spent on refining the main apparatus, where every improvement will be seen in the data, and benefit the accuracy of the experiment.

References

- [1] Amazon, Wathai, 20 July 2019. [Online]. Available: https://www.amazon.com/Wathai-Controller-Receiver-Playstation-Component/dp/B07VYGQPCZ?ref_=ast_sto_dp&th=1. [Accessed 5 September 2022].
- [2] R. Bryant, O. Sanni, E. Moore, M. Bundy and A. Johnson, "Taylor & Francis Online," 20 May 2014. [Online]. Available: <https://www.tandfonline.com/doi/full/10.1080/10962247.2014.881437>. [Accessed 20 September 2022].
- [3] E. L. M. PE, "Equal Area vs. Log-Tchebycheff," *HPAC Engineering*, pp. 26-31, 1999.
- [4] S. Denki, "Training, Fan Basics," [Online]. Available: https://techcompass.sanyodenki.com/en/training/cooling/fan_basic/001/index.html . [Accessed 5 September 2022].
- [5] M. Burke, "Analog Dialogue," February 2004. [Online]. Available: <https://www.analog.com/en/analog-dialogue/articles/how-to-control-fan-speed.html>. [Accessed 8 September 2022].
- [6] Cooler Master, [Online]. Available: <https://www.coolermaster.com/catalog/coolers/case-fan/silent-fan-120-si1/>.
- [7] Accutron, "FlowTrax Ultrasonic airflow monitor," [Online]. Available: <https://accutroninstruments.com/flowtrax-ultrasonic-airflow-monitor/>. [Accessed 11 September 2022].
- [8] R. Cressall, R. Schaap, D. R. Neal, A. Mychkovsky, J. Charonko and B. L. Smith, "Accuracy of volumetric flow rate inflow/outflow measurement by integrating PIV velocity fields," 23 September 2020. [Online]. Available: <https://iopscience.iop.org/article/10.1088/1361-6501/ab9bb7>. [Accessed 8 September 2022].
- [9] G. J. Matthews, "How to Determine Air Flow," Airflow Developments Limited.
- [10] Airflow Developments Limited, "Airflow Grids," [Online]. Available: http://www.techmark.co.in/pfma/brochures/airflow_grids.pdf. [Accessed 8 September 2020].
- [11] M. Arlit, E. Schleicher and U. Hampel, "Thermal Anemometry Grid Sensor," 19 July 2017. [Online]. Available: <https://www.mdpi.com/1424-8220/17/7/1663/htm>. [Accessed 8 September 2022].

- [12] M. R. Ahemad and C. Zhou, "Estimation of volumetric flow rate through a circular duct: Equal area versus Log-Tchebycheff," University of Windsor, Windsor, Ontario, Canada, 2005.
- [13] F. Yao, S. Li, Z. Sun, T. Zhou and Z. Dong, "Diameter bisection: An effective traverse method in Pitot tube based flow measurement," in *2016 35th Chinese Control Conference (CCC)*, Chengdu, 2016.
- [14] Testo, "Testo 420 flow hood," [Online]. Available: <https://static-int.testo.com/media/54/96/f0a8e975911f/Testo-420-Flow-Hood-Data-Sheet-US.pdf>. [Accessed 8 September 2022].
- [15] Omega, "Air Flow Measurement Instruments: How Precise and Accurate?," [Online]. Available: <https://www.omega.co.uk/technical-learning/how-precise-and-accurate-are-air-flow-measurement-instruments.html>. [Accessed 8 September 2022].
- [16] Dwyer Instruments, "Duct Traversing for Average Air Velocity and Air Volume," 18 October 2017. [Online]. Available: <http://blog.dwyer-inst.com/2017/10/18/duct-traversing-for-average-air-velocity-and-air-volume/#sthash.8cx0KtTb.dpbs>. [Accessed 17 September 2022].